Research Article
Cancer

JOURNAL
OF HEPATOLOGY

Immunogenomic landscape of hepatocellular carcinoma with immune cell stroma and EBV-positive tumor-infiltrating lymphocytes

Graphical abstract

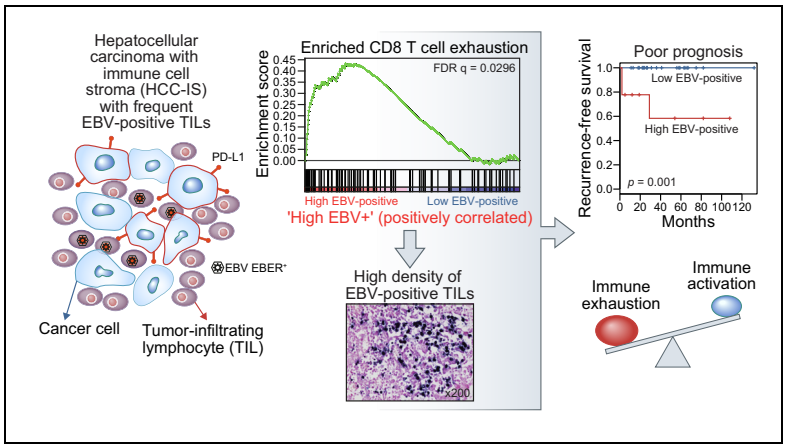

Highlights

- EBV positivity in CD20-positive tumor-infiltrating lymphocytes was present in over 70% of HCC-IS.
- HCC-IS lacked *CTNNB1* mutations and exhibited increased global DNA hypermethylation.
- Both PD-1 and PD-L1 in tumor-infiltrating lymphocytes, and PD-L1 in tumor cells were overexpressed in HCC-IS.
- HCCs with high EBV positivity, paradoxically, were associated with a poor prognosis.
- HCCs with high EBV positivity exhibited increased levels of functionally exhausted CD8 T cells.

Authors

Hyo Jeong Kang, Ji-Hye Oh, Sung-Min Chun, ..., Ju Hyun Shim, Chang Ohk Sung, Eunsil Yu

Correspondence

s5854@amc.seoul.kr (J.H. Shim), co.sung@amc.seoul.kr (C.O. Sung), esyu@amc.seoul.kr (E. Yu)

Lay summary

Hepatocellular carcinomas with histologic evidence of abundant immune cell infiltration are characterized by frequent activation of Epstein-Barr virus in tumor-infiltrating lymphocytes and less aggressive clinical behavior. However, a high density of Epstein-Barr virus-positive tumor-infiltrating lymphocytes is associated with inferior prognostic outcomes, possibly as a result of immune escape due to significant CD8 T cell exhaustion.

http://dx.doi.org/10.1016/j.jhep.2019.03.018

Research Article
Cancer

JOURNAL OF HEPATOLOGY

Immunogenomic landscape of hepatocellular carcinoma with immune cell stroma and EBV-positive tumor-infiltrating lymphocytes

Hyo Jeong Kang[1,†], Ji-Hye Oh[2,†], Sung-Min Chun[1,3], Deokhoon Kim[1,3], Yeon-Mi Ryu[4], Hee Sang Hwang[1], Sang-Yeob Kim[4,5], Jihyun An[6,7,8], Eun Jeong Cho[2], Hyeonjin Lee[2], Ju Hyun Shim[6,9,*], Chang Ohk Sung[1,2,3,*], Eunsil Yu[1,9,*]

[1]*Department of Pathology, Asan Medical Center, University of Ulsan College of Medicine, Seoul, Republic of Korea;* [2]*Department of Medical Science, Asan Medical Institute of Convergence Science and Technology, University of Ulsan College of Medicine, Seoul, Republic of Korea;* [3]*Center for Cancer Genome Discovery, Asan Institute for Life Science, Asan Medical Center, Seoul, Republic of Korea;* [4]*Asan Institute for Life Science, Asan Medical Center, Seoul, Republic of Korea;* [5]*Department of Convergence Medicine, University of Ulsan College of Medicine, Asan Medical Center, Seoul, Republic of Korea;* [6]*Department of Gastroenterology, Asan Medical Center, University of Ulsan College of Medicine, Seoul, Republic of Korea;* [7]*Department of Bio and Brain Engineering, Korea Advanced Institute of Science and Technology, Daejeon, Republic of Korea;* [8]*Department of Gastroenterology and Hepatology, Hanyang University of Medicine, Guri, Republic of Korea;* [9]*Asan Liver Center, Asan Medical Center, University of Ulsan College of Medicine, Seoul, Republic of Korea*

Background & aims: The immunogenomic characteristics of hepatocellular carcinomas (HCCs) with immune cell stroma (HCC-IS), defined histologically, have not been clarified. We investigated the clinical and molecular features of HCC-IS and the prognostic impact of Epstein-Barr virus (EBV) infection.

Methods: We evaluated 219 patients with conventional HCC (C-HCC) and 47 with HCC-IS using *in situ* hybridization for EBV, immunohistochemistry, multiplex immunofluorescence staining, and whole exome and transcriptome sequencing. Human leukocyte antigen types were also extracted from the sequencing data. Genomic and prognostic parameters were compared between HCC-IS and C-HCC. *Results:* CD8 T cell infiltration was more frequent in HCC-IS than C-HCC (mean fraction/sample, 22.6% *vs.* 8.9%, false discovery rate q <0.001), as was EBV positivity in CD20-positive tumor-infiltrating lymphocytes (TILs) (74.5% *vs.* 4.6%, p <0.001). *CTNNB1* mutations were not identified in any HCC-IS, while they were present in 24.1% of C-HCC (p = 0.016). Inhibitory and stimulatory immune modulators were expressed at similar levels in HCC-IS and EBV-positive C-HCC. Global hypermethylation, and expression of PD-1 and PD-L1 in TILs, and PD-L1 in tumors, were also associated with HCC-IS (p <0.001), whereas human leukocyte antigen type did not differ according to HCC type or EBV positivity. HCC-IS was an independent factor for favorable recurrence-free survival (adjusted hazard ratio [aHR] 0.23; p = 0.002). However, a subgroup of tumors with a high density of EBV-positive TILs had poorer recurrence-free (aHR 25.48; p <0.001) and overall (aHR 9.6; p = 0.003) survival, and significant enrichment of CD8 T cell exhaustion signatures (q = 0.0296).

Conclusions: HCC-IS is a distinct HCC subtype associated with a good prognosis and frequent EBV-positive TILs. However, paradoxically, a high density of EBV-positive TILs in tumors is associated with inferior prognostic outcomes. Patients with HCC-IS could be candidates for immunotherapy.

Lay summary: Hepatocellular carcinomas with histologic evidence of abundant immune cell infiltration are characterized by frequent activation of Epstein-Barr virus in tumor-infiltrating lymphocytes and less aggressive clinical behavior. However, a high density of Epstein-Barr virus-positive tumor-infiltrating lymphocytes is associated with inferior prognostic outcomes, possibly as a result of immune escape due to significant CD8 T cell exhaustion.

Introduction

Hepatocellular carcinomas (HCCs) are biologically heterogeneous at the molecular level, and thus diverse molecular subgroups based on large-scale exome or transcriptome profiling have been identified.[1–4] This oncologic background may prevent novel molecular-targeted agents from significantly improving survival rates in patients with HCC.[5] Immune checkpoint inhibitors, including anti-programmed cell death 1 (PD-1) and anti-programmed cell death 1 ligand 1 (PD-L1), are emerging as potential anti-HCC agents,[6,7] and a unique immune class specific for HCC was recently defined based on gene expression profiling of tumor tissues.[8–10]

However, the immunogenic subgroup of HCC defined by gene expression profiling may not always correspond to the immunogenic subgroup defined histologically. In fact, immune cells act in a variety of locations and under various conditions, such as on the periphery of tumors, and as secondary inflamma-

Keywords: Hepatocellular carcinoma; Immune; Epstein-Barr virus; Sequencing.
Received 18 October 2018; received in revised form 12 February 2019; accepted 14 March 2019; available online 29 March 2019

* Corresponding authors. Address: Department of Gastroenterology, Asan Medical Center, University of Ulsan College of Medicine, 88, Olympic-ro 43-gil, Songpa-gu, Seoul, 05505, Republic of Korea; Tel.: +82-2-3010-3190, fax: +82-2-485-5782 (J.H. Shim), or Center for Cancer Genome Discovery, Asan Institute for Life Science, and Department of Pathology, Asan Medical Center, University of Ulsan College of Medicine, 88 Olympic-ro 43 gil, Songpa-gu, Seoul 05505, Republic of Korea; Tel.: +82 2 3010 4546, fax: +82 2 472 7898 (C.O. Sung), or Department of Pathology, Asan Medical Center, University of Ulsan College of Medicine, 88 Olympic-ro 43 gil, Songpa-gu, Seoul 05505, Republic of Korea; Tel.: +82 2 3010 4552, fax: +82 2 472 7898 (E. Yu).
E-mail addresses: s5854@amc.seoul.kr (J.H. Shim), co.sung@amc.seoul.kr (C.O. Sung), esyu@amc.seoul.kr (E. Yu).
† Hyo Jeong Kang and Ji-Hye Oh contributed equally to this study.

tory reactions to bile duct obstruction and/or ischemic tumor cell necrosis, so that histologic evaluation of tumor tissue is useful for identifying true intra-tumor immune cell infiltration.[11] Therefore, a combined analysis of histology and gene expression in tumors and their microenvironments should be able to identify more reliable immunogenic subtypes of HCCs. Moreover, the subgroup of HCC with marked immune cell infiltration defined histologically has been reported to have favorable prognosis.[12,13] However, the microenvironmental and genomic features of this HCC subgroup with immune cell stroma (HCC-IS) have not been identified.

Among many tumors with marked lymphoid cell infiltration, a few epithelial carcinomas, such as lymphoepithelioma-like gastric cancers and head & neck undifferentiated carcinomas, develop in response to Epstein-Barr virus (EBV), and those tumors typically contain a lymphoid-rich stroma.[14,15] EBV positivity in these EBV-driven epithelial carcinomas was found only in the epithelial cancer cells, not the lymphocytic cells.[14,15] However, there have been no convincing reports of HCC infected by EBV, and moreover the status of EBV in tumor-infiltrating lymphocytes (TILs) is unclear. Considering that EBV-infected B lymphocytes can induce cellular immune responses,[16] identifying EBV particles in TILs and determining their clinical role may be keys to understanding the pathogenesis of the HCC-IS subtype.

Herein, we have identified the HCC-IS subtype by microscopic evaluation in a large HCC cohort primarily undergoing curative resection. We have also investigated the genomic and immunomolecular characteristics of the subgroup, focusing particularly on the EBV status of TILs and its prognostic relevance.

Materials and methods

Patients and samples

We searched the electronic medical records of Asan Medical Center, Seoul, Korea between 2005 and 2016 for patients who had received their first curative resection for HCC, to identify HCC-IS. Sixty patients were initially selected, and all selected patients had descriptions of lymphoid stroma, lymphoid reaction, or lymphoid hyperplasia in their pathology reports. A hematoxylin and eosin (H&E) slide review excluded 5 patients with predominantly neutrophil infiltration, a hemorrhage-associated lymphoid reaction, or severe chronic hepatitis-associated lymphoid infiltration. Twenty patients with necrosis-associated lymphoid infiltration preoperatively treated with transarterial chemoembolization or radiofrequency ablation were also excluded. We initially also used 231 patients from our previous study for the conventional HCC (C-HCC) group;[4] these patients had also received a first curative resection for HCC. However, after reviewing the H&E slides, 12 of the cases (5.2%) were reclassified as the HCC-IS subtype. Therefore, 47 patients were finally classified as having HCC-IS and the remaining 219 patients as having C-HCC. We defined the selection criteria for HCC-IS in detail as follows: an HCC with prominent intra-tumoral immune cell stroma with/without lymphoid follicles; these should not be associated with i) predominant portal area inflammation and/or active cirrhosis (cirrhosis with variable inflammation and liver cell damage along the fibrotic band); ii) hepatolithiasis and/or cholangitis; iii) immune cell infiltration associated with secondary degeneration such as tumor necrosis, hemorrhage, or fibrosis; and iv) major infiltration of non-lymphocyte immune cells such as neutrophils, eosinophils or plasma cells associated with an infectious response or a different immune environment.[17,18]

The procedure for selecting the included cases is summarized in Fig. S1. This retrospective study was approved by the Institutional Review Board of Asan Medical Center. The institution review board waived the requirement to obtain informed consent by anonymized retrospective study.

Immunohistochemical staining and evaluation

Formalin-fixed paraffin-embedded (FFPE) tissues (n = 266) were immunohistochemically stained with antibodies for PD-1, PD-L1, 5-methylcytosine (5MeC), and acetylated histone H3 lysine 9 (AcH3K9), using a Bench Mark XT automatic immunostaining device according to the manufacturer's instructions. PD-L1 expression in tumor cells (PDL1-Tumor) and in TILs (PDL1-TIL) and PD-1 expression in TILs (PD1-TIL) were scored using an immunoreactivity scoring system (IRS) based on the percentage and staining intensity of stained cells (Table S1). Intra-tumoral immune cells with an IRS score ≥1 for PD1-TIL or PDL1-TIL, and an IRS score of ≥3 for PDL1-Tumor were defined as positive for the corresponding marker. 5MeC and AcH3K9 expressions in the nucleus of tumor cells were evaluated, and background lymphocytes served as positive controls. The percentage of stained tumor cells (0–100%) was used as an estimate of 5MeC and AcH3K9 expression.

EBV-encoded RNA-*in situ* hybridization

EBV-encoded RNA-*in situ* hybridization (EBER-ISH) was performed using a Bench Mark XT autostainer (Ventana Medical Systems) with a Ventana ISH iVIEW Blue Detection Kit (Ventana Medical Systems) in all FFPE tissue samples. The density of EBV-positive TILs was measured as the number of EBV-positive TILs per high power field (EBV/HPF). High and low EBV positivity were defined as >10 EBV/HPF, and present but ≤10 EBV/HPF, respectively.

Multiplex immunofluorescence staining and analysis

Multiplex immunofluorescence staining was performed with an Opal™ 7-color Automation immunohistochemistry (IHC) Kit with a Leica Bond Rx™ Automated Stainer on the 44 HCC-IS samples. The expression of PD-1, PD-L1, CD8, and CD3 was visualized with a tyramide signal amplification (TSA®) Plus Opal system. The expression of CD3 and CD8 was quantified as positive cell density (cell number per mm^2), which was measured as cell number per field/0.36 in the Opal system.[19] The expression of PD-1 and PD-L1 was evaluated as percentages of positive cells (0–100%).

DNA sequencing and data processing

All fresh tissues for next-generation sequencing were obtained from the Bio-Resource Center in the Asan Medical Center. We used whole exome sequencing (WES) data newly performed on fresh tumor and matched surrounding non-neoplastic tissues from 8 HCC-IS, combined with binary alignment map and mutation annotation file data for 206 cases with matched RNA sequencing (RNA-seq) data from our previous study.[4]

Somatic copy number analysis

We used a Affymetrix CytoScan HD Array (Affymetrix, Santa Clara, CA, USA) for the 206 cases from our previous report[4] and binary alignment map files for the 8 newly added cases.

RNA sequencing and data processing

RNA-seq data were generated from 214 fresh tissues available in the Bio-Resource Center of our center. The normalized gene expression data were deposited in GEO (https://www.ncbi.nlm.nih.gov/geo) (Accession number, GSE124751 and GSE124752).

Profiling of tumor-infiltrating immune cells

CIBERSORT[20] was used to quantify absolute proportions as the immune scores of the various tumor-infiltrating immune cell types in tumor tissues from the normalized gene expression data generated by RNA-seq of the 214 samples. The total immune score was defined as the sum of the estimated immune scores for each cell type. Immune phenotypes were classified based on the previously defined immune[8] and stromal[21] classifiers with a false discovery rate (FDR) threshold of 5% defining significance of prediction.

Gene set enrichment and pathway analyses

To conduct gene set enrichment and pathway analyses, we used V6.1 dataset from the Molecular Signatures Database.[22,23] To assess the gene set enrichment scores of individual samples, gene set variation analysis (GSVA) scores were calculated from the normalized gene expression data using GSVA v1.24.2.[24]

Human leukocyte antigen typing

Human leukocyte antigen (HLA) class I alleles were predicted at 4-digit resolution using the RNA-seq data of the 214 samples. The WES data of the 8 pairs of tumors and matched non-tumors newly generated in this study were used to check the consistency of the HLA typing results between the datasets.

Statistical analysis

Overall survival (OS) was measured from the day of tumor resection to the date of death or last follow-up. Recurrence-free survival (RFS) was assessed from the day of tumor resection to disease recurrence or last follow-up.

For further details regarding the materials and methods used, please refer to the CTAT table.

Results

Characteristics of HCC-IS and EBV positivity in the tumor stroma

We first compared the clinicopathological features of HCC-IS (n = 47) with those of C-HCC (n = 219) (Table S2). HCC-IS patients were older ($p = 0.027$), and had smaller tumors ($p < 0.001$) and a higher Edmondson-Steiner grade measured by the worst grade ($p = 0.006$). Rare architectural patterns ($p < 0.001$), and rare cell types ($p = 0.005$), were more frequent in HCC-IS. Lymphoid follicles were observed only in the HCC-IS ($p < 0.001$). Representative histological images are shown in Fig. 1A and S2A-D.

We performed a quantitative analysis of the stromal areas occupied by immune cells using the Opal system (Fig. 1B). The area of the immune cell stroma was significantly greater in HCC-IS ($p < 2.2e-16$, Fig. 1C). Mean stromal area was 27.2% (SD ± 8.1%) in HCC-IS, and no difference in the mean stromal area was observed between the tumor margin (28.2 ± 7.5%; red area in Fig. 1B) and the central tumor area (26.1 ± 9.7%; yellow area in Fig. 1B). Although an enlarged immune stromal area was also present in 28C-HCC, this was always associated with active cirrhosis (n = 10, Fig. 1C), necrosis (n = 11), hemorrhage (n = 6), or stones (n = 1), based on the H&E slides. The best estimate of the cut-off percentage of immune stromal area for discriminating between C-HCC and HCC-IS was 19.5% (Fig. 1D). Patients with HCC-IS had a better RFS than those with C-HCC ($p < 0.001$, Fig. 1E), and HCC-IS was an independent prognostic factor for RFS (adjusted hazard ratio [aHR] 0.23; 95% CI 0.09–0.59; $p = 0.0021$) (Table S3). The patients with HCC-IS tended to survive longer, although this was not statistically significant ($p = 0.155$, Fig. 1E).

We evaluated EBV positivity using EBER-ISH on whole slide sections of all 266 samples, and compared the status of tumor cells and intra-/extra-tumoral immune cells. EBV positivity was detected in 74.5% of HCC-IS and 4.6% of C-HCC ($p < 0.001$; Fig. 1F), and the mean numbers of EBV-positive TILs/HPF per sample were 10.5 ± 26.4, and 0.2 ± 1.0, respectively ($p < 2.2e-16$; Fig. 1G). Only intra-tumoral immune cells were positive for EBV; no EBV positivity was detected in tumor cells or extra-tumoral lymphoid cells. Ten tumors in the HCC-IS group had a relatively high density of EBV positivity (>10 positive cells/HPF), while only 1 in the C-HCC group did (Fig. 1G, right side). EBV positivity was only present in CD20-positive TILs and was not observed in CD68-positive macrophages (Fig. 1H and S2E).

Genomic alterations characteristic of HCC-IS

The somatic mutations and mutational signatures of HCC-IS (n = 19) were compared with those of C-HCC (n = 195). The landscape of gene mutations and mutational signatures, along with associated clinicopathological features including EBV status, are summarized in Fig. 2A. An interesting finding was that *CTNNB1* mutations were encountered more frequently in C-HCC (47/195), than in HCC-IS (0/19, $p = 0.016$). The COSMIC signature 22, which is associated with aristolochic acid and present in urothelial carcinomas and liver cancers,[25] was rarer in HCC-IS than in C-HCC (Fig. 2A and S3), but the overall mutation burden did not differ between the 2 groups (median value 1.86 mutations/Mb in HCC-IS *vs.* 2.02 mutations/Mb in C-HCC; $p = 0.105$). In terms of somatic copy number variation, 1q21, 1q44, 8q23, 8q24, and 11q13 amplifications; and 10q22, 10q26, 13q13, 13q14, 16q24, and 17p13 deletions were significantly associated with C-HCC, whereas 10q11 amplifications and 18p11 deletions were associated with HCC-IS (Fig. 2B and S4).

Profiling of immune cells in the tumor microenvironment

We investigated the tumor-infiltrating immune cell types in the HCCs using CIBERSORT[20] and the RNA-seq data from the 214 samples (Fig. 3). The total immune score, the sum of 22 leukocyte cell fractions, was significantly higher in HCC-IS than in C-HCC (mean score 0.796 *vs.* 0.297; FDR q = 6.85e-08; Table S4). More precisely, the immune scores of 11 of the 22 immune cell types, including B cells, CD8 T cells, CD4 memory T cells, and macrophages, were significantly higher in HCC-IS than in C-HCC (Fig. 3A and Table S4). The correlation between CD8 T cell expression assessed by the CIBERSORT and Opal methods was significant in the analysis of 16 of 19 HCC-IS cases, excluding 3 without matched RNA-seq data ($p = 0.014$ and rho = 0.605; Fig. 3B), suggesting that immune cell profiling based on RNA-seq data is reliable. Pathway analysis revealed that CD28 costimulatory signaling, T cell receptor signaling, IL2 signaling, and Toll receptor signaling pathways were upregulated in HCC-IS compared to C-HCC (Fig. 3C).

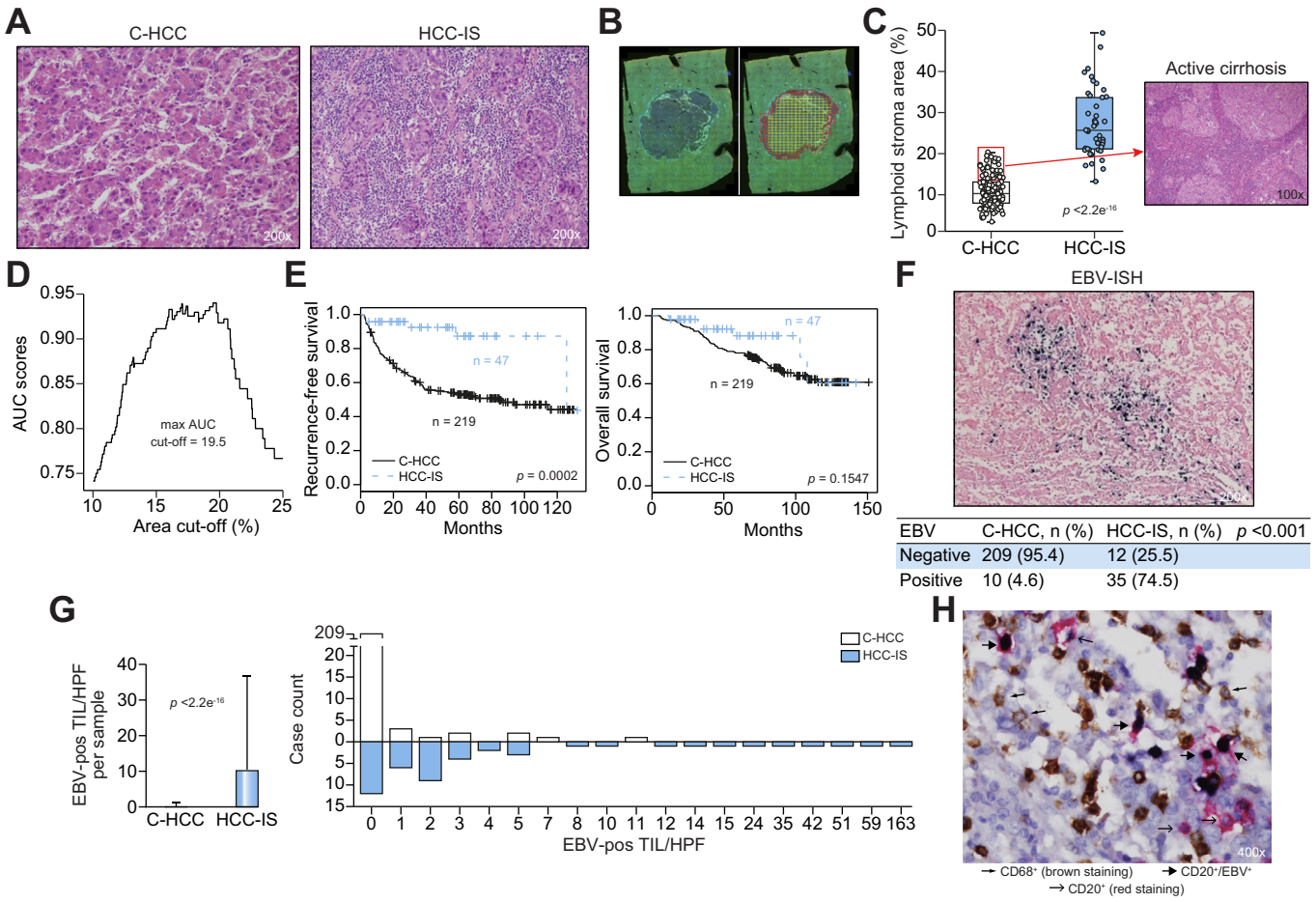

Fig. 1. Histological characteristics of HCC-IS and C-HCC. (A) Histological slides of HCC-IS and C-HCC showing marked intra-tumoral immune cell infiltration in the HCC-IS. (H&E stain, ×200). (B) Measurement of lymphoid stromal areas using Opal imaging (red, peripheral area of the tumor; yellow, central area of the tumor). (C) Difference in mean lymphoid stromal area (%) between HCC-IS and C-HCC (*t* test). Some C-HCC had an increased lymphoid stromal area due to active cirrhosis (H&E stain, ×100). (D) The estimated cut-off percentage of lymphoid stromal area for discriminating C-HCC and HCC-IS. (E) Survival differences between the C-HCC and HCC-IS groups (log-rank test). (F) EBV detection in tumor-infiltrating immune cells using EBER-ISH (Fisher's exact test). (G) Frequency and distribution of EBV-positive TILs per sample in C-HCC and HCC-IS (Wilcoxon rank-sum test). (H) Triple staining with EBV-ISH (dark blue, nuclear staining), anti-CD20 (red, arrow head), and anti-CD8 (brown, thin arrows) reveals that EBVs are present in CD20-positive B lymphocytes (thick arrows). AUC, area under the curve; C-HCC, conventional HCC; EBER, EBV-encoded RNA; EBV, Epstein-Barr virus; H&E, hematoxylin & eosin; HCC, hepatocellular carcinoma; HCC-IS, HCC subgroup with immune cell stroma; HPF, high power field; ISH, *in situ* hybridization; TILs, tumor-infiltrating lymphocytes. (This figure appears in colour on the web.)

Next, we investigated the relative proportions of different immune cell types in subgroups according to HCC type and EBV positivity (Table S5). The greatest proportional difference in a cell type between C-HCC and HCC-IS was observed for CD8 T cells (8.9% *vs.* 22.6%, $p = 1.18e-07$ and FDR q = 1.30e-06; Fig. 4A and Table S6). The proportion of CD8 T cells did not differ from that of CD4 T cell in HCC-IS (22.6% *vs.* 17.1%; $p = 0.1301$), whereas it was lower in C-HCC (8.9% *vs.* 20.1%, $p < 0.001$; Fig. 4A). A similar finding was obtained in the HCC subtypes according to EBV positivity (Fig. 4B and S5A). However, there was no significant difference in the proportions of macrophages, another major immune cell type, between the 2 HCC subtypes (38.8% for C-HCC *vs.* 33.5% for HCC-IS; $p = 0.063$ and FDR q = 0.166; Table S6). The proportions of CD4 T cells, CD8 T cells, and macrophages did not differ according to EBV positivity in any of the subgroups stratified by HCC type (Fig. 4C and 4D), which suggests that immune cell profiles based on quantitative measurements are associated more with HCC type than with EBV positivity.

Global methylation and histone acetylation patterns

We evaluated global methylation and histone acetylation patterns in tumor cells according to HCC type and EBV positivity, using IHC of 5MeC and AcH3K9.[26] More pronounced global hypermethylation was identified in HCC-IS compared to C-HCC, with mean percentages of stained cells per sample of 84.5% *vs.* 58.7%, respectively ($p = 4.4e-07$; Fig. 4E). However, we found no significant difference in DNA methylation pattern according to EBV positivity (Fig. 4E). These findings point to a relationship between immune cell infiltration into the tumor microenvironment and DNA methylation of the cancer cells. Global histone acetylation patterns did not differ between the groups (Fig. S5B).

Associations between HCC type or EBV positivity and expression of PD-1 and PD-L1

We evaluated PD-L1, PD-1, CD3, and CD8 expression by Opal in 44 HCC-IS; and PD-L1 and PD-1 expression by IHC in the entire 266 cases. Significant correlations were observed between the

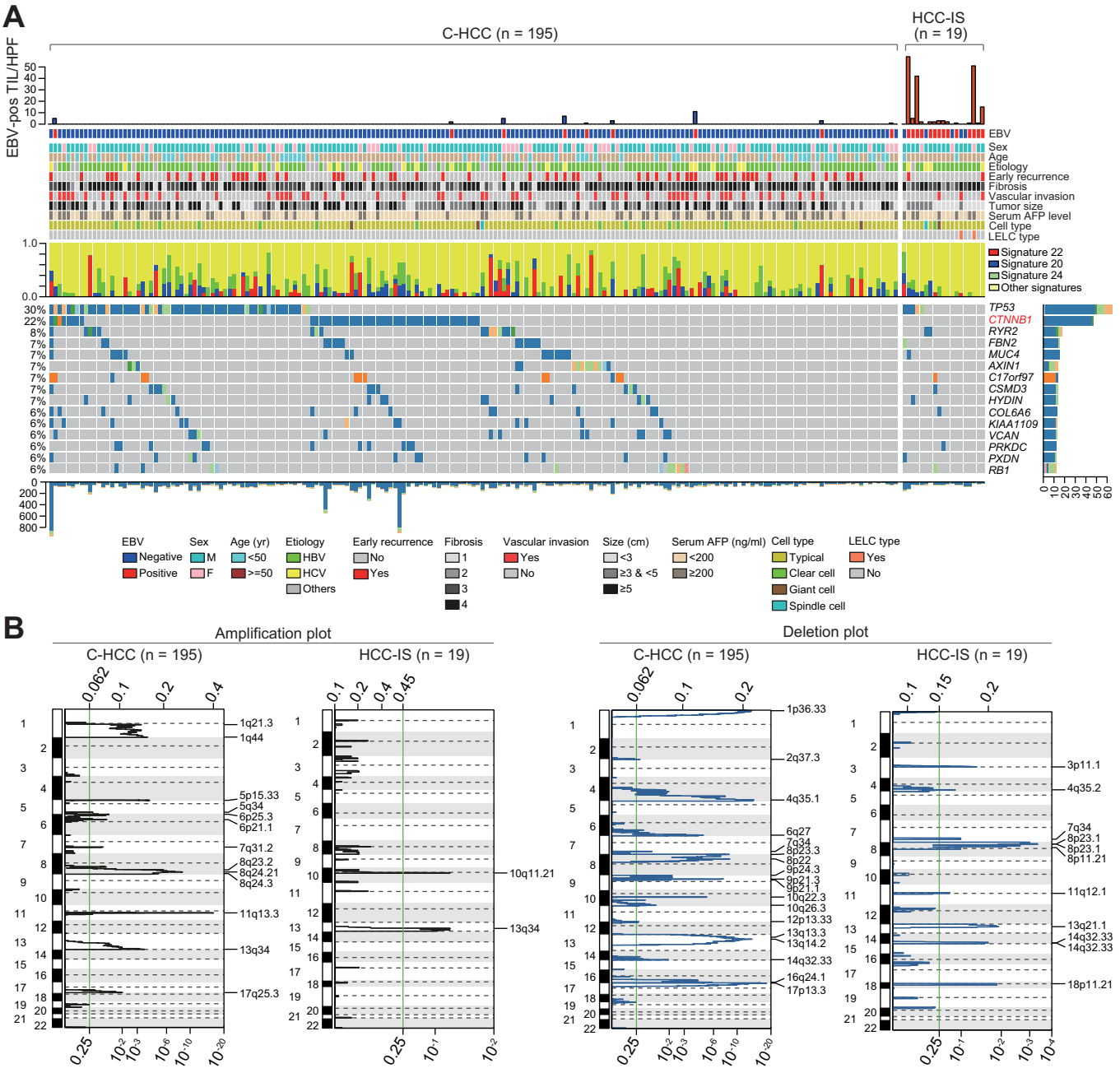

Fig. 2. Genetic characteristics of HCC-IS and C-HCC. (A) Landscapes of somatic mutations and mutational signatures in HCC-IS and C-HCC, along with various clinicopathological factors. (B) Profiles of somatic copy number alterations in HCC-IS and C-HCC. AFP, alpha-fetoprotein; C-HCC, conventional HCC; HCC, hepatocellular carcinoma; HCC-IS, HCC subgroup with immune cell stroma; LELC, lymphoepithelioma-like carcinoma. (This figure appears in colour on the web.)

IHC and Opal data for PD1-TIL ($p = 5.9e-09$), PDL1-TIL ($p = 0.0038$), and PDL1-Tumor ($p = 2.4e-07$) (Fig. 5A). Based on IRS scores by IHC, PDL1-TIL, PDL1-Tumor, and PD1-TIL were significantly overexpressed in HCC-IS (Fig. 5B). In particular, 66.0% (31 out of 47) of HCC-IS were positive for PDL1-Tumor (IRS score ≥3), but only 22.4% (49 out of 219) of C-HCC. The IHC expression patterns of PD-L1 and PD-1 in all 266 cases are shown in Fig. 5C. Based on the Opal data for the 44 HCC-IS, PDL1-Tumor was significantly correlated with intra-tumoral CD8 T cell density ($p = 0.013$); both PDL1-TIL and PDL1-Tumor positivity were closely correlated with PD1-TIL ($p = 5.89e-08$ and $p = 6.58e-08$, respectively; Fig. S6). The number of EBV-positive TILs was also correlated with PDL1-Tumor positivity by Opal (rho = 0.4 and $p = 0.0034$; Fig. 5D).

Immune checkpoint-related gene expression according to HCC type and EBV positivity

The median normalized expression levels of various immune checkpoint-related genes[27] were significantly different across the 4 subgroups: EBV-negative C-HCC (subgroup 1, n = 186); EBV-positive C-HCC (subgroup 2, n = 9); EBV-negative HCC-IS (subgroup 3, n = 5); and EBV-positive HCC-IS (subgroup 4, n = 14) (Fig. 6A). Specifically, the median levels of 23 inhibitory genes and 37 stimulatory genes were similar in subgroups 2, 3,

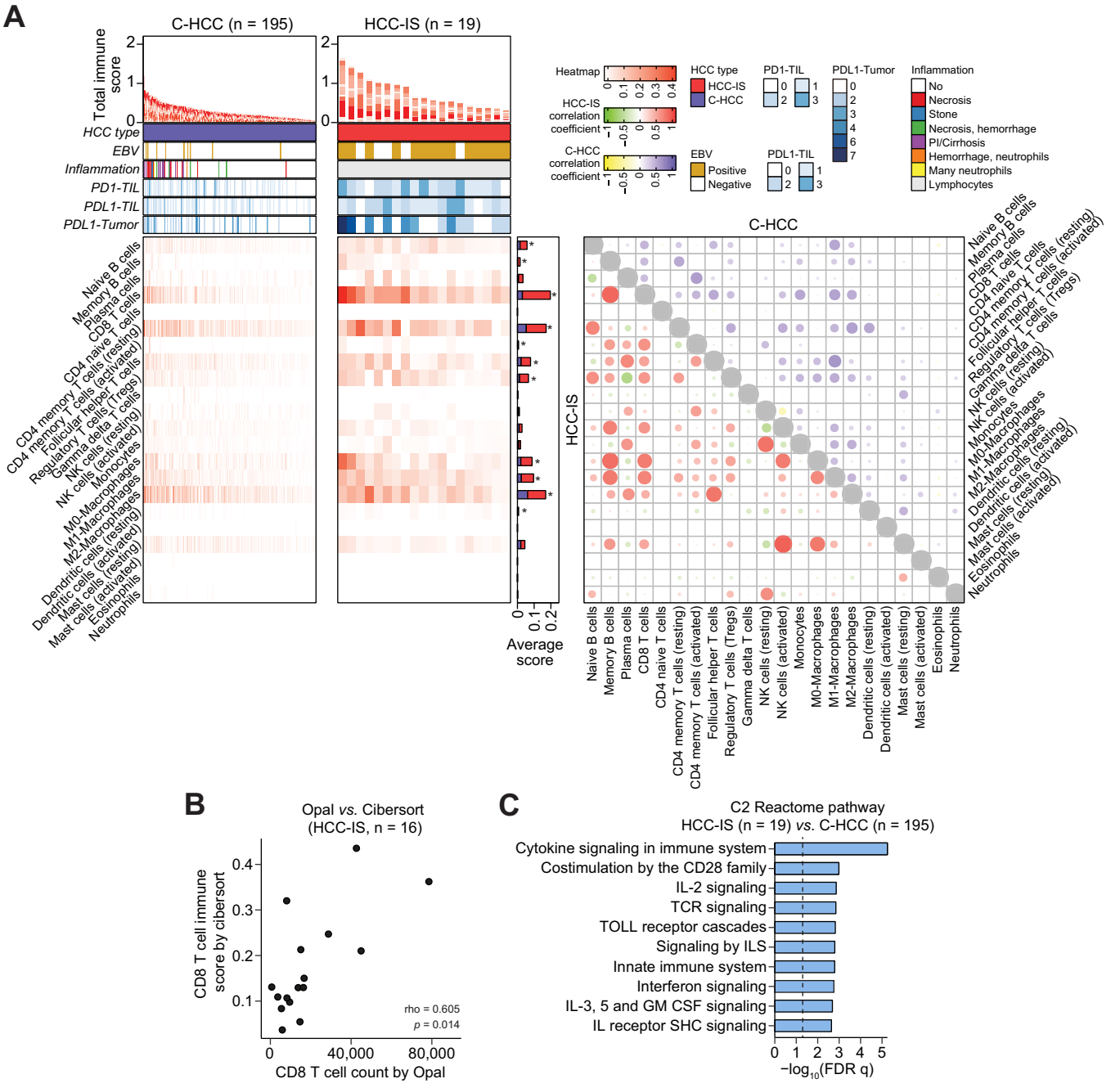

Fig. 3. Microenvironmental immune cell profiling of HCC-IS and C-HCC. (A) Estimated absolute scores for each immune cell type by CIBERSORT and PD1-TIL, PDL1-TIL, and PDL1-Tumor immunostaining in C-HCC and HCC-IS. Differences in cell type numbers between the 2 groups are marked with a * indicating FDR q <0.05 (Wilcoxon rank-sum test). (B) Spearman correlations between immune scores estimated by CIBERSORT using RNA sequencing data, and by Opal using CD8 T cells, in 16 HCC-IS. (C) Significantly upregulated pathway in HCC-IS compared to C-HCC using the C2 Reactome database. Black dot bar indicates gene set enrichment analysis FDR q <0.05. C-HCC, conventional HCC; FDR, false discovery rate; HCC, hepatocellular carcinoma; HCC-IS, HCC subgroup with immune cell stroma; PD-1, programmed cell death 1; PD-L1, programmed cell death 1 ligand 1; PI, portal inflammation; TILs, tumor-infiltrating lymphocytes. (This figure appears in colour on the web.)

and 4, and significantly greater than in subgroup 1 (Fig. 6B), suggesting that EBV-positive C-HCC was also similar with HCC-IS in terms of its immunomodulatory gene expression pattern. HLA class I and II genes were highly expressed in HCC (Fig. 6A). We also evaluated HLA class I molecular types (both genotype and supertype) from the RNA-seq data (n = 214). When we compared the relevant results using the tumor DNA and matched non-tumor DNA data, along with the tumor RNA-seq data for 8 cases, the HLA typing results were consistent (Fig. S7). The frequencies of HLA class I molecular types among all HCCs are shown in Fig. 6C. These frequencies agreed well with those previously reported in 5,082 Koreans.[28] No significant disparities in HLA supertype or genotype (FDR q >0.05) were found according to EBV status and HCC type after adjusting nominal p values (Fig. 6D and S8). In a survival analysis by HLA type, supertype B58 displayed inferior OS and similar PFS to the other types ($p = 0.008$ and $p = 0.092$, respectively; Fig. 6E).

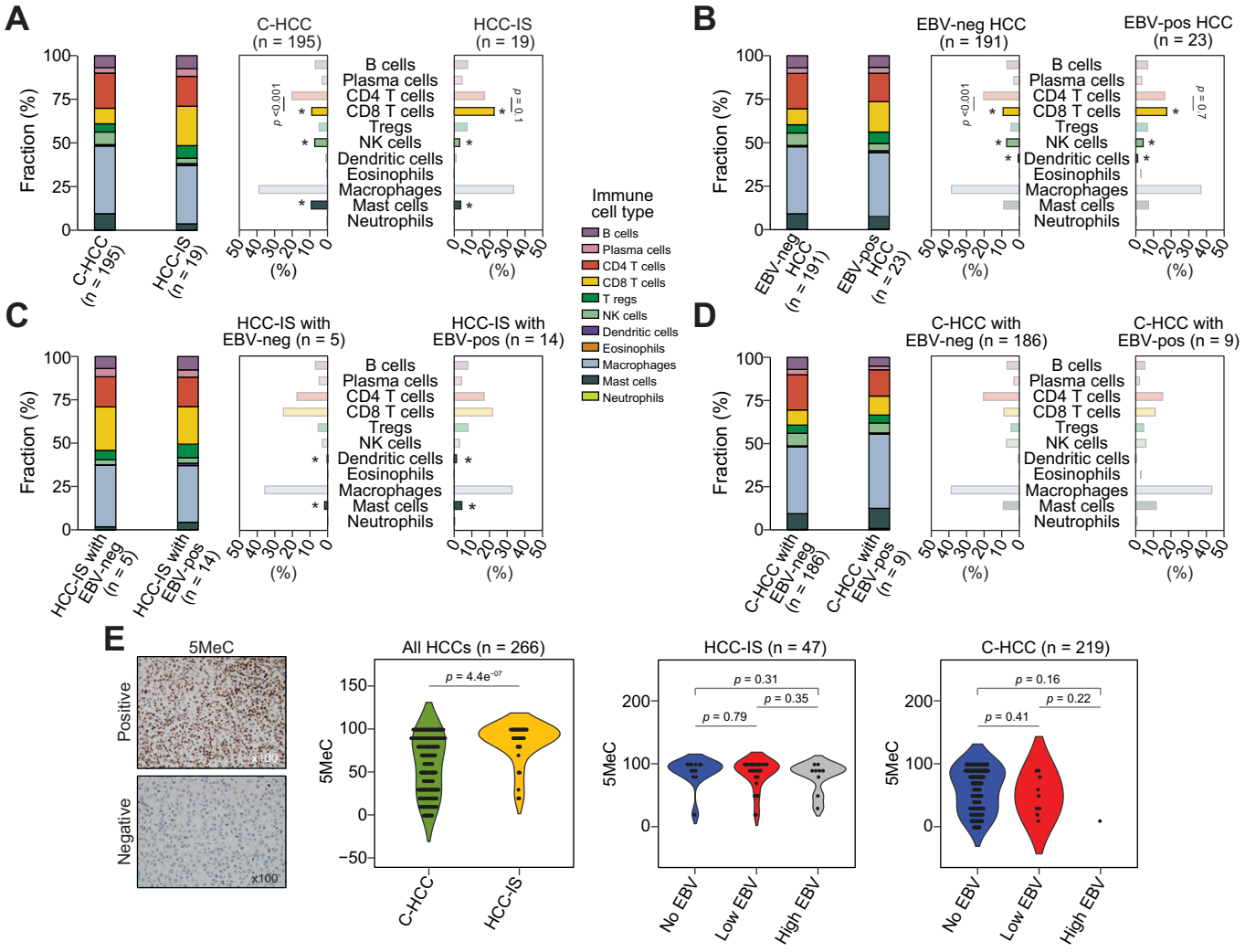

Fig. 4. Relative immune cell proportions and methylation patterns by HCC type and EBV positivity. Relative proportions of immune cell types according to (A) HCC type (n = 214); (B) EBV positivity (n = 214); (C) EBV positivity in HCC-IS (n = 23); and (D) EBV positivity in C-HCC (n = 191) (Wilcoxon rank-sum test). (E) Differences in global DNA methylation pattern by HCC type and EBV status (Wilcoxon rank-sum test). *Indicates FDR q <0.05 between the groups. C-HCC, conventional HCC; EBV, Epstein-Barr virus; FDR, false discovery rate; HCC, hepatocellular carcinoma; HCC-IS, HCC subgroup with immune cell stroma; NK, natural killer. (This figure appears in colour on the web.)

Potential clinical implications of EBV positivity in HCC

EBV positivity was associated with HCC type (HCC-IS *vs.* C-HCC), age, and various immune cell types in univariate logistic regression analysis; however only HCC type and age were significant in multivariate analysis (Fig. 7A and Table S7). Kaplan-Meier survival analysis revealed that EBV positivity was associated with better RFS ($p = 0.0016$), but not OS ($p = 0.9997$) (Fig. 7B). However, we noted a different survival effect according to the density of EBV-positive TILs in HCCs: high EBV positivity was significantly associated with poorer RFS and OS in the totality of cases, as well as in each HCC subtype (Fig. 7C and S9A). This association was independent of other clinicopathological variables (aHR 25.4 for RFS, $p < 0.001$; aHR 9.6 for OS, $p = 0.003$; Tables S8 and S9). The HR for RFS increased with the density of EBV-positive TILs, with a plateau at >5 EBV-positive TILs/HPF (Fig. 7D).

Association between high EBV positivity and increased CD8 T cell exhaustion

We further analyzed microenvironmental immune status using the RNA-seq data because the strongly EBV-positive cases were associated with poor prognosis in spite of the infiltration of sufficient immune cells into the tumors. Based on the RNA-seq data (n = 214), the expression of 252 genes (FDR q <0.05; Fig. 7E) was related to the density of EBV-positive TILs by Spearman's correlation analysis, and using the 252 gene set, the immunodeficiency pathway defined by KEGG (Kyoto Encyclopedia of Genes and Genomes) was significantly enriched in HCCs that were highly positive for EBV (FDR q = 1.3e-09; Fig. 7F and S9B). We further classified our HCCs (n = 214) into the 4 subgroups using both immune[8] and stromal[21] classifiers (Fig. S10, and Tables S10 and S11): immune-exhausted (n = 53, 24.8%); immune-active (n = 18, 8.4%); immune-desert (n = 62, 29.0%); and not-assigned (n = 81, 37.9%) subgroups were identified and their characteristic features are summarized in Fig. 8A. The immune-exhausted phenotype was more common in the high EBV-positive group (3 out of 4, 75%) than in the low EBV-positive group (5 out of 10, 50%) (Fig. 8B and S11). In addition, a significantly higher CD8 T cell exhaustion score (Table S12), as assessed by GSVA analysis,[29] was obtained in the high EBV-positive group than in the rest of the groups in an analysis of the totality of cases ($p = 3.23e-08$; Fig. 8C), as well

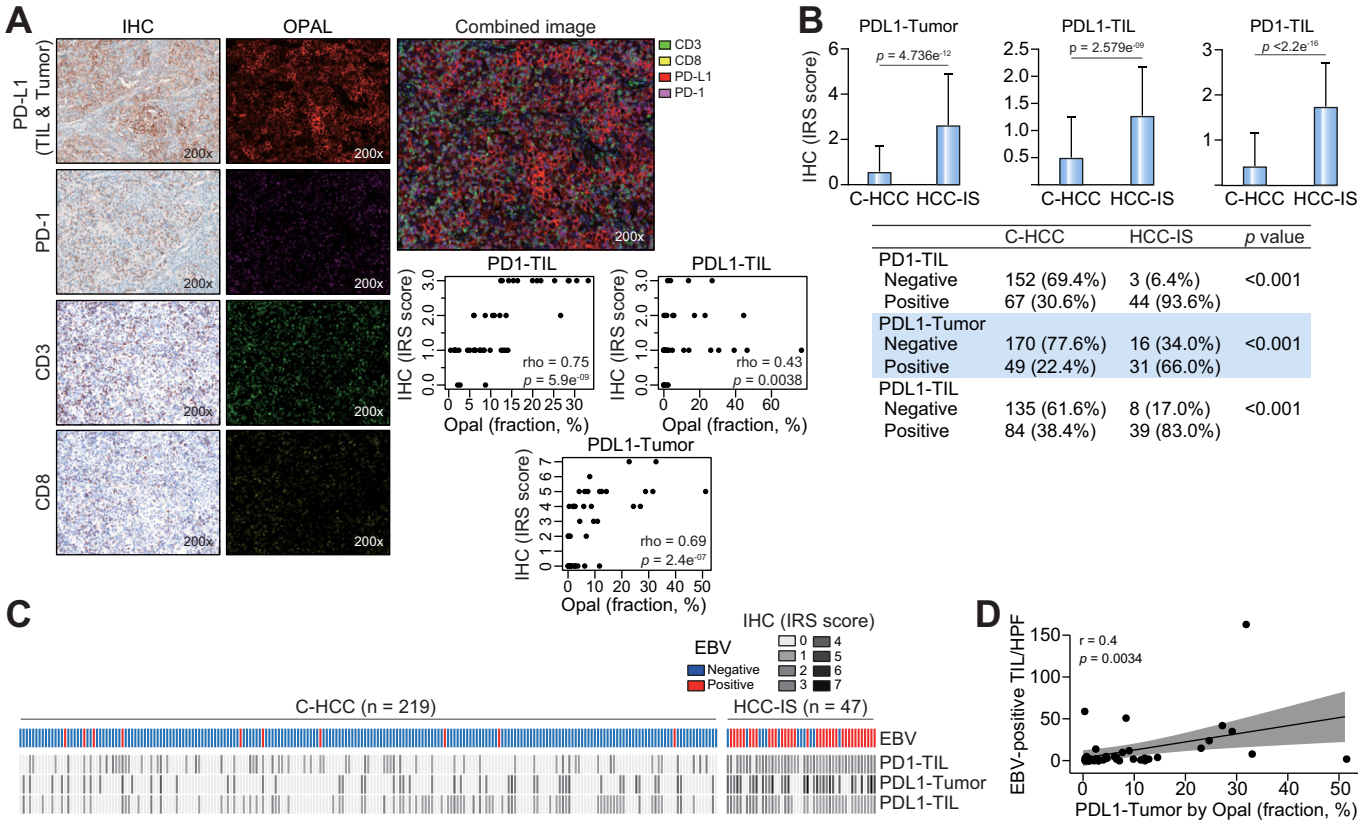

	C-HCC	HCC-IS	*p* value
PD1-TIL			
Negative	152 (69.4%)	3 (6.4%)	<0.001
Positive	67 (30.6%)	44 (93.6%)	
PDL1-Tumor			
Negative	170 (77.6%)	16 (34.0%)	<0.001
Positive	49 (22.4%)	31 (66.0%)	
PDL1-TIL			
Negative	135 (61.6%)	8 (17.0%)	<0.001
Positive	84 (38.4%)	39 (83.0%)	

Fig. 5. Patterns of expression of PD-1 and PD-L1 in HCC-IS and C-HCC. (A) Correlations between the staining results of IHC and Opal for PD-1, PD-L1, CD3, and CD8 in 44 HCC-IS (Spearman correlation test). (B) Differences in IHC expression of PD-1 and PD-L1 between HCC-IS (n = 47) and C-HCC (n = 219) in tumors and TILs (Wilcoxon rank-sum test & Fisher's exact test). (C) PD-1 and PD-L1 IHC expression in HCC-IS and C-HCC. (D) Correlation between EBV-positive TILs/HPF and density of PD-L1-positive tumor cells measured by Opal (Spearman correlation test). C-HCC, conventional HCC; EBV, Epstein-Barr virus; FDR, false discovery rate; HCC, hepatocellular carcinoma; HCC-IS, HCC subgroup with immune cell stroma; HPF, high power field; IHC, immunohistochemistry; IRS, immunoreactivity scores; PD-1, programmed cell death 1; PD-L1, programmed cell death 1 ligand 1; TIL, tumor-infiltrating lymphocytes. (This figure appears in colour on the web.)

as in a limited subgroup of 19 HCC-IS ($p = 0.021$; Fig. 8D). The upregulated CD8 T cell exhaustion signature was stronger in the high EBV-positive HCC-IS group (n = 4), than in the low EBV-positive HCC-IS group (n = 10) (FDR q = 0.0296; Fig. 8D).

Discussion

HCCs with abundant TILs have been consistently described as having good prognosis[12,13,30]; however, little is known about the type of HCC involved. Based on our histological and immunogenomic results, we could define the unique characteristics of the HCC-IS category as follows: i) marked intra-tumoral CD8 TILs; ii) favorable recurrence outcomes; iii) high frequency of intra-tumoral EBV-positive TILs; iv) strong expression of immune checkpoint proteins such as PD-1 and PD-L1; v) rarity of *CTNNB1* mutations; and vi) increased global hypermethylation.

We also found that HCC-IS were genetically different from C-HCC in terms of their somatic mutation patterns, especially of *CTNNB1* mutations. The Wnt/β-catenin pathway is an important oncogenic signaling pathway related to immune evasion.[31]. Activation of the Wnt/β-catenin pathway causes extinction of T cells from the microenvironment, and *CTNNB1*-mutated HCCs display reduced immune cell infiltration.[8,31–33] These previous findings agree well with the absence of *CTNNB1* mutations in the current HCC-IS series.

Recently, DNA hypermethylation has been reported as an epigenetic consequence of EBV infection in gastric cancer.[34] However, although global hypermethylation was more prevalent in HCC-IS than C-HCC, there was no significant effect of EBV positivity *per se* on the global methylation level in our HCC samples. This difference may be related to the fact that in the HCCs, the EBV was present in TILs not in the actual tumor cells, in contrast to the situation in gastric cancer.

In the present study, CD8 TILs were the dominant subset of immune cells in the HCC-IS subtype, and EBV was found only in the fraction of CD20-positive TILs. EBV infections in the tumor microenvironment affected clinical outcomes differently depending on the histological virus burden, indicating a potential prognostic effect in the post-carcinogenic period rather than a causal role in hepatocarcinogenesis.

While HCC-IS had a favorable prognosis, those with a high density of EBV-positive TILs had poorer outcomes regardless of their HCC type. Further analysis based on immune and stromal classifiers indicated that the HCCs with high EBV burdens were enriched for functionally defective exhausted T cells, which can attenuate anti-tumor immunity in various cancers.[35] This observation may explain the paradoxical effect of density of EBV-positive TILs on the prognosis of patients with HCC.

Although a pathogenic role of EBV infection in the immunological milieu of HCC cannot be clearly identified from our

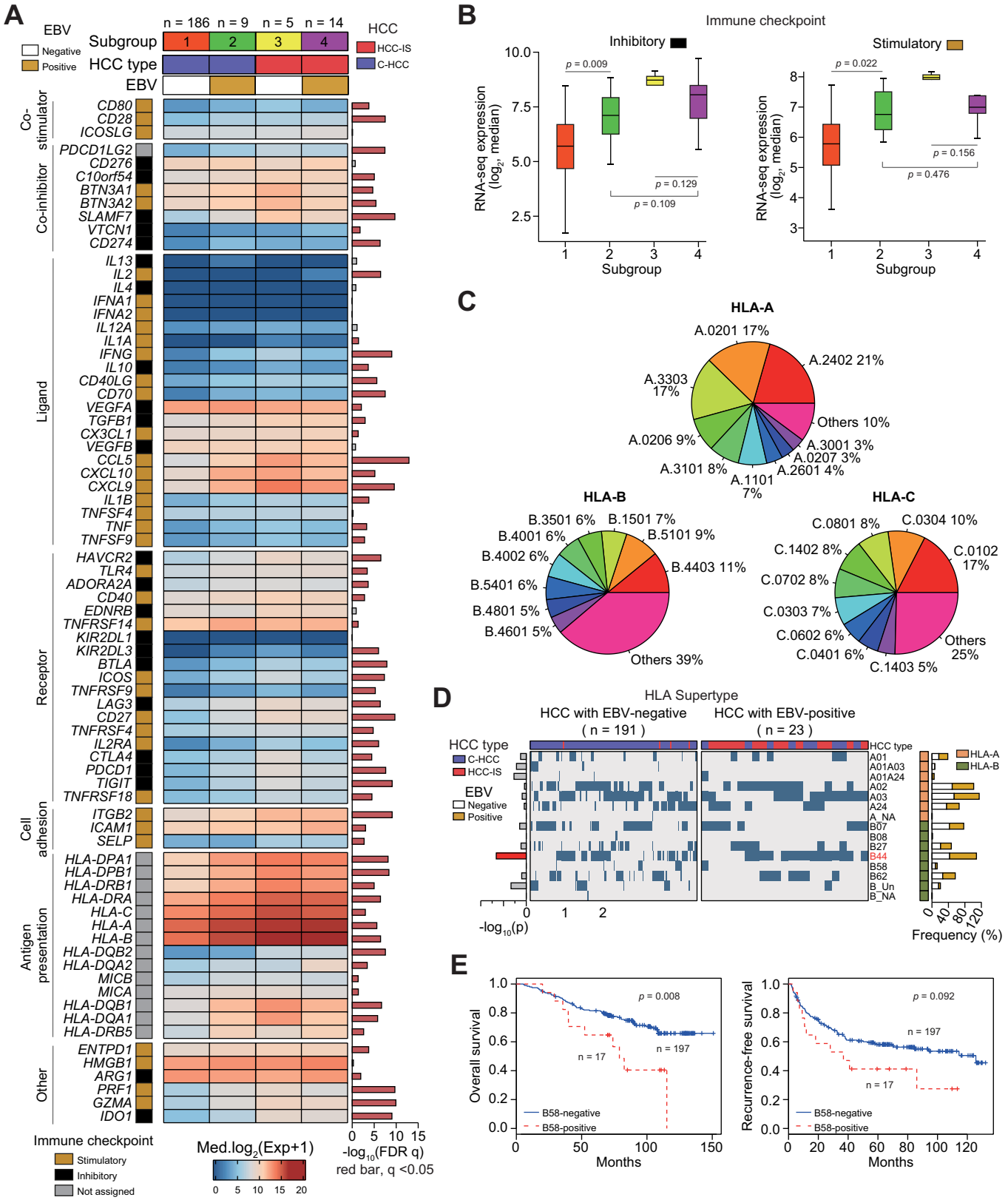

Fig. 6. Patterns of expression of immune checkpoint-related genes. (A) Expression of immune checkpoint-related genes according to the 4 subgroups classified by HCC type and EBV positivity (1-way ANOVA). (B) Median expression levels of 23 inhibitory and 37 stimulatory genes across the 4 subgroups (Wilcoxon rank-sum test). (C) High-resolution typing and frequencies of HLA class I. (D) Frequency of HLA supertypes according to EBV positivity (Fisher's exact test). (E) Survival of patients with (n = 17) and without B58 supertype (n = 197) (log-rank test). C-HCC, conventional HCC; EBV, Epstein-Barr virus; HCC, hepatocellular carcinoma; HCC-IS, HCC subgroup with immune cell stroma; HLA, human leukocyte antigen; RNA-seq, RNA sequencing. (This figure appears in colour on the web.)

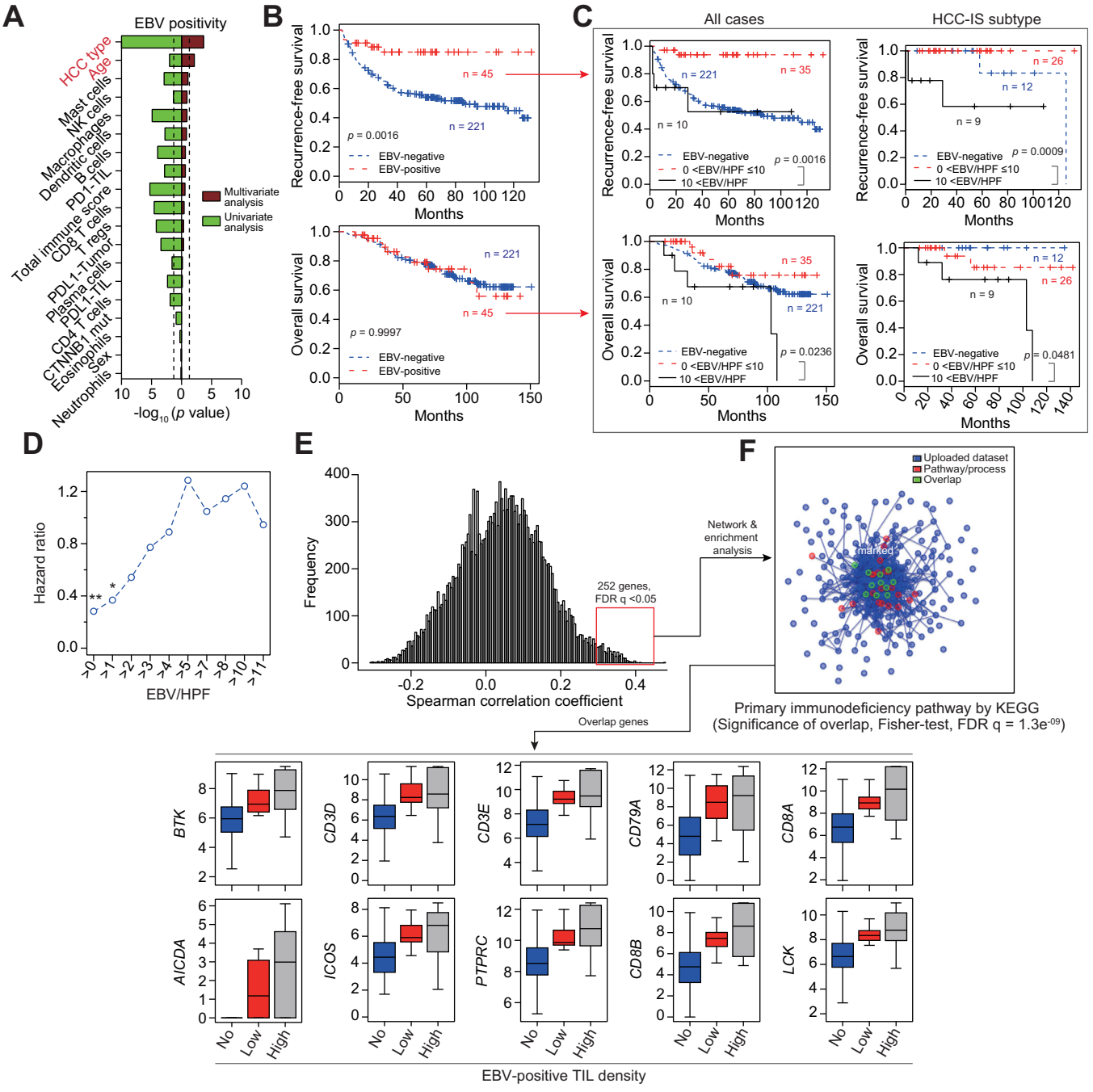

Fig. 7. Clinical relevance of the density of EBV-positive TILs, and related pathways. (A) Parameters associated with EBV positivity using a logistic regression model. (B) Survival curves of patients with EBV-positive (n = 45) and EBV-negative HCCs (n = 221) (log-rank test). (C) Survival according to density of EBV-positive TILs (EBV/HPF) in the complete HCC set (n = 266) and in the HCC-IS subtype (n = 47) (log-rank test). (D) Dependence of HRs on EBV/HPF. (E) Histogram of Spearman correlation coefficients between expression of genes and EBV/HPF, and the 252 genes with significant correlations (FDR q <0.05). (F) The primary immunodeficiency pathway defined by KEGG is significantly enriched in the 252 gene set (Fisher's exact test). EBV, Epstein-Barr virus; FDR, false discovery rate; HCC, hepatocellular carcinoma; HCC-IS, HCC subgroup with immune cell stroma; HPF, high power field; HR, hazard ratio; KEGG, Kyoto Encyclopedia of Genes and Genomes; NK, natural killer; TIL, tumor-infiltrating lymphocytes. (This figure appears in colour on the web.)

results, such infection seems to contribute to immune cell infiltration as a result of the induced activation of lymphocytes and macrophages.[16,36] Conversely, T cell exhaustion due to a prolonged anti-cancer inflammatory response may lead to reactivation of EBV from a chronic latent state.

In terms of application, our data suggest a potential clinical use of EBV positivity for stratifying patients with HCC with regard to prognosis and treatment options. Indeed, high- level expression of immunomodulator genes in EBV-positive HCC may presage good responses to the immune checkpoint inhibitors.

Although we did not examine EBV serology in this study, East Asia including Korea is an EBV endemic area, and almost the entire population has a chronic latent infection.[37] Therefore, the status of EBV serology may have had no impact on the results of this study.

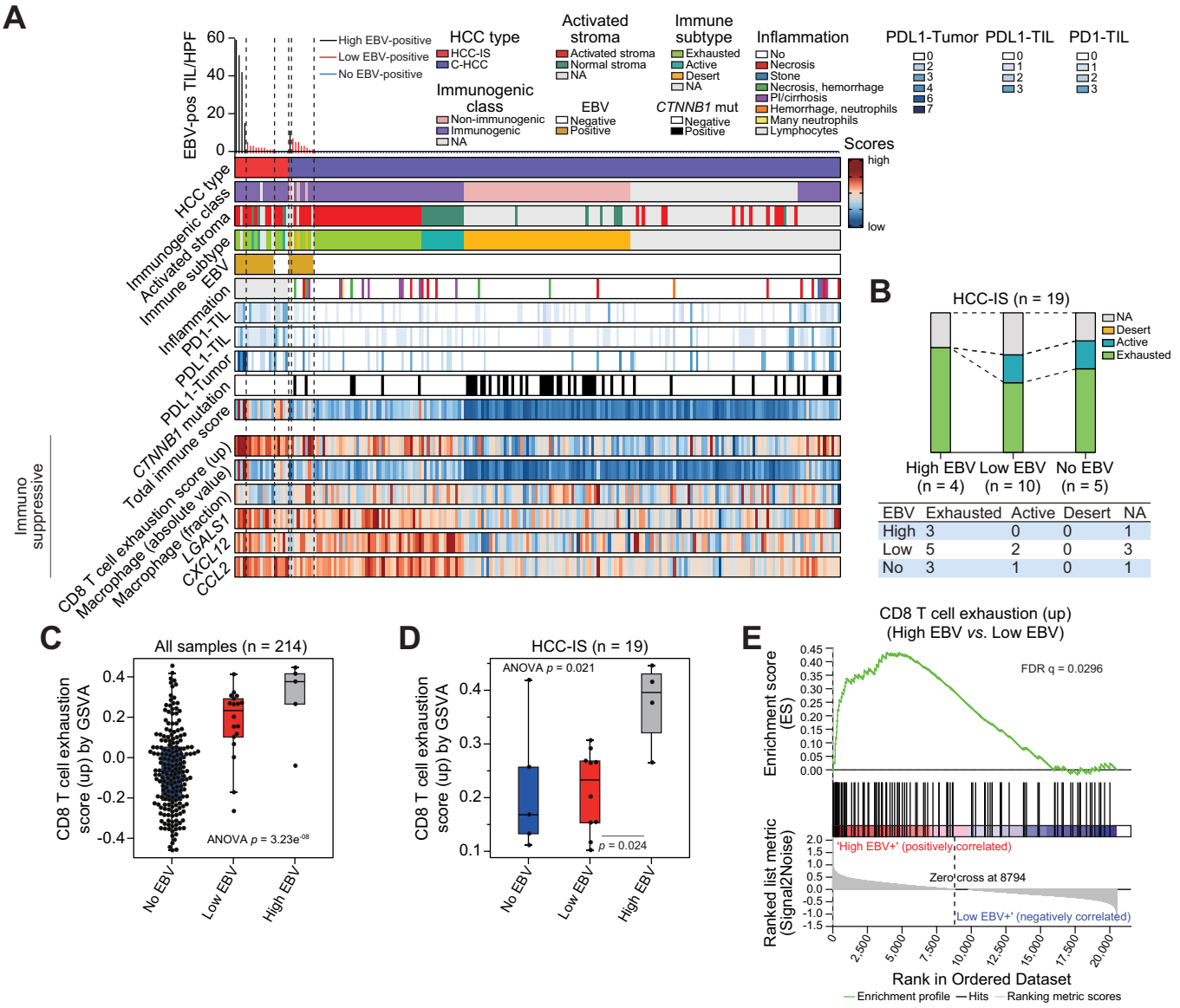

Fig. 8. Classification of the complete set of HCC samples (n = 214) using immune and stromal classifiers. (A) Various parameters and classified immune subtypes. (B) Frequency of immune subtypes as a function of the density of EBV-positive TILs (EBV/HPF) in HCC-IS (n = 19). (C) CD8 T cell exhaustion scores are highest in tumors with high EBV positivity in the analysis of the entire set (1-way ANOVA), and (D) in the analysis of the HCC-IS subtype (1-way ANOVA & Wilcoxon rank-sum test). (E) Gene set enrichment scores of CD8 T cell exhaustion signatures between the high EBV- (n = 4) and low EBV-positive HCC-IS groups (n = 10). HPF, high power field; PI, portal inflammation; TIL, tumor-infiltrating lymphocytes. EBV, Epstein-Barr virus; GSVA, gene set variation analysis; HCC, hepatocellular carcinoma; HCC-IS, HCC subgroup with immune cell stroma; HPF, high power field; HR, hazard ratio; TIL, tumor-infiltrating lymphocytes. (This figure appears in colour on the web.)

In conclusion, HCC-IS has unique prognostic, genomic, and pathologic features, and is associated with a specific cancer microenvironment containing a high frequency of EBV-positive TILs. Exhausted immune function may contribute at least in part to the negative effect of high density of EBV-positive TILs on survival. Our findings identify a novel HCC entity that is essential for immunohistological classification and accurate management of patients with HCC.

Financial support

This work was supported by the Basic Science Research Program through NRFK (NRF-2017R1C1B2009899 and NRF-2017R1E1A1A01074298), the Bio & Medical Technology Development Program of the National Research Foundation of Korea (NRFK) (NRF-2017M3A9G5061671 and NRF-2017M3A9G5061673), grant 2017–660 from the Asan Institute for Life Sciences of Asan Medical Center, Korea, and the Technology Innovation Program for Fostering New Post-Genome Industry funded by the Ministry of Trade, Industry & Energy (MOTIE) (#10067796 and #10067407) funded by the Korean government.

Conflicts of interest

All authors declare no potential conflicts of interest.

Please refer to the accompanying ICMJE disclosure forms for further details.

Authors' contributions

E Yu, CO Sung, and JH Shim conceived the project and provided leadership. CO Sung, HJ Kang, and E Yu designed the study. CO Sung and JH Oh analyzed the data and interpreted the results. JH Shim and HS Hwang contributed to the analysis of the data. JH Shim and E Yu contributed to the interpretation of the results. JH Oh and CO Sung designed and made all figures and tables. JH Shim contributed to the production of figures and tables. HJ Kang, CO Sung, E Yu, JH Shim, SM Chun, JH Oh, DH Kim, YM Ryu, SY Kim, J An, EJ Cho, and H Lee contributed to designing and performing the experiments and generating the data. CO Sung, JH Shim, JH Oh, E Yu, and HJ Kang wrote the manuscript.

Acknowledgements

The production of some of the RNA sequencing data was supported by Sanofi-Aventis. We thank Dr. Heounjeong Go and Dr. Jaenam Ko for the triple and double staining using EBV-ISH. We thank the optical imaging core facility at the ConveRgence mEDIcine research cenTer (CREDIT), Asan Medical Center for support and instrumentation. This work was supported by the Basic Science Research Program through NRFK (NRF-2017R1C1B2009899 and NRF-2017R1E1A1A01074298), the Bio & Medical Technology Development Program of the National Research Foundation of Korea (NRFK) (NRF-2017M3A9G5061671 and NRF-2017M3A9G5061673), grant 2017-660 from the Asan Institute for Life Sciences of Asan Medical Center, Korea, and the Technology Innovation Program for Fostering New Post-Genome Industry funded by the Ministry of Trade, Industry & Energy (MOTIE) (#10067796 and #10067407) funded by the Korean government.

Supplementary data

Supplementary data to this article can be found online at https://doi.org/10.1016/j.jhep.2019.03.018.

References

Author names in bold designate shared co-first authorship

[1] The Cancer Genome Atlas Research Network Wheeler David A, Roberts Lewis R. Comprehensive and Integrative Genomic Characterization of Hepatocellular Carcinoma. Cell 2017;169:1327–1341, e1323.
[2] **Boyault S**, **Rickman DS**, **de Reynies A**, Balabaud C, Rebouissou S, Jeannot E, et al. Transcriptome classification of HCC is related to gene alterations and to new therapeutic targets. Hepatology (Baltimore, MD) 2007;45:42–52.
[3] Hoshida Y, Nijman SM, Kobayashi M, Chan JA, Brunet JP, Chiang DY, et al. Integrative transcriptome analysis reveals common molecular subclasses of human hepatocellular carcinoma. Cancer Res 2009;69:7385–7392.
[4] **Ahn SM**, **Jang SJ**, **Shim JH**, **Kim D**, Hong SM, Sung CO, et al. Genomic portrait of resectable hepatocellular carcinomas: implications of RB1 and FGF19 aberrations for patient stratification. Hepatology (Baltimore, MD) 2014;60:1972–1982.
[5] Thillai K, Ross P, Sarker D. Molecularly targeted therapy for advanced hepatocellular carcinoma - a drug development crisis? World J Gastrointestinal Oncol 2016;8:173–185.
[6] **Ohaegbulam KC**, **Assal A**, Lazar-Molnar E, Yao Y, Zang X. Human cancer immunotherapy with antibodies to the PD-1 and PD-L1 pathway. Trends Mol Med 2015;21:24–33.
[7] Kudo M. Immune checkpoint inhibition in hepatocellular carcinoma: basics and ongoing clinical trials. Oncology 2017;92(Suppl 1):50–62.
[8] Sia D, Jiao Y, Martinez-Quetglas I, Kuchuk O, Villacorta-Martin C, Castro de Moura M, et al. Identification of an immune-specific class of hepatocellular carcinoma, based on molecular features. Gastroenterology 2017;153:812–826.
[9] Carone C, Olivani A, Dalla Valle R, Manuguerra R, Silini EM, Trenti T, et al. Immune gene expression profile in hepatocellular carcinoma and surrounding tissue predicts time to tumor recurrence. Liver Cancer 2018;7:277–294.
[10] Kurebayashi Y, Ojima H, Tsujikawa H, Kubota N, Maehara J, Abe Y, et al. Landscape of immune microenvironment in hepatocellular carcinoma and its additional impact on histological and molecular classification. Hepatology (Baltimore, MD) 2018;68:1025–1041.
[11] Hayashi A, Shibahara J, Misumi K, Arita J, Sakamoto Y, Hasegawa K, et al. Histologic assessment of intratumoral lymphoplasmacytic infiltration is useful in predicting prognosis of patients with hepatocellular carcinoma. PLoS ONE 2016;11 e0155744.
[12] Shirabe K, Matsumata T, Maeda T, Sadanaga N, Kuwano H, Sugimachi K. A long-term surviving patient with hepatocellular carcinoma including lymphocytes infiltration–a clinicopathological study. Hepatogastroenterology 1995;42:996–1001.
[13] Wada Y, Nakashima O, Kutami R, Yamamoto O, Kojiro M. Clinicopathological study on hepatocellular carcinoma with lymphocytic infiltration. Hepatology (Baltimore, MD) 1998;27:407–414.
[14] Thompson MP, Kurzrock R. Epstein-Barr virus and cancer. Clin Cancer Res 2004;10:803–821.
[15] Gullo I, Oliveira P, Athelogou M, Goncalves G, Pinto ML, Carvalho J, et al. New insights into the inflamed tumor immune microenvironment of gastric cancer with lymphoid stroma: from morphology and digital analysis to gene expression. Gastric Cancer 2018.
[16] Young LS, Rickinson AB. Epstein-Barr virus: 40 years on. Nat Rev Cancer 2004;4:757–768.
[17] Gregory AD, Houghton AM. Tumor-associated neutrophils: new targets for cancer therapy. Cancer Res 2011;71:2411–2416.
[18] Nathan C. Neutrophils and immunity: challenges and opportunities. Nat Rev Immunol 2006;6:173–182.
[19] **Cho CJ**, **Kang HJ**, **Ryu YM**, Park YS, Jeong HJ, Park YM, et al. Poor prognosis in Epstein-Barr virus-negative gastric cancer with lymphoid stroma is associated with immune phenotype. Gastric Cancer 2018;21:925–935.
[20] **Newman AM**, **Liu CL**, Green MR, Gentles AJ, Feng W, Xu Y, et al. Robust enumeration of cell subsets from tissue expression profiles. Nat Methods 2015;12:453–457.
[21] Moffitt RA, Marayati R, Flate EL, Volmar KE, Loeza SG, Hoadley KA, et al. Virtual microdissection identifies distinct tumor- and stroma-specific subtypes of pancreatic ductal adenocarcinoma. Nat Genet 2015;47:1168–1178.
[22] **Mootha VK**, **Lindgren CM**, Eriksson KF, Subramanian A, Sihag S, Lehar J, et al. PGC-1alpha-responsive genes involved in oxidative phosphorylation are coordinately downregulated in human diabetes. Nat Genet 2003;34:267–273.
[23] **Subramanian A**, **Tamayo P**, Mootha VK, Mukherjee S, Ebert BL, Gillette MA, et al. set enrichment analysis: a knowledge-based approach for interpreting genome-wide expression profiles. Proc Natl Acad Sci USA 2005;102:15545–15550.
[24] Hanzelmann S, Castelo R, Guinney J. GSVA: gene set variation analysis for microarray and RNA-seq data. BMC Bioinf 2013;14:7.
[25] Alexandrov LB, Nik-Zainal S, Wedge DC, Aparicio SA, Behjati S, Biankin AV, et al. Signatures of mutational processes in human cancer. Nature 2013;500:415–421.
[26] Barbisan F, Mazzucchelli R, Santinelli A, Stramazzotti D, Scarpelli M, Lopez-Beltran A, et al. Immunohistochemical evaluation of global DNA methylation and histone acetylation in papillary urothelial neoplasm of low malignant potential. Int J Immunopathol Pharmacol 2008;21:615–623.
[27] Thorsson V, Gibbs DL, Brown SD, Wolf D, Bortone DS, Ou Yang TH, et al. The immune landscape of cancer. Immunity 2018;48, 812–830. e814.
[28] **Park HJ**, **Kim YJ**, Kim DH, Kim J, Park KH, Park JW, et al. HLA allele frequencies in 5802 Koreans: varied allele types associated with SJS/TEN according to culprit drugs. Yonsei Med J 2016;57:118–126.
[29] Wherry EJ, Ha SJ, Kaech SM, Haining WN, Sarkar S, Kalia V, et al. Molecular signature of CD8+ T cell exhaustion during chronic viral infection. Immunity 2007;27:670–684.
[30] Emile JF, Adam R, Sebagh M, Marchadier E, Falissard B, Dussaix E, et al. Hepatocellular carcinoma with lymphoid stroma: a tumour with good prognosis after liver transplantation. Histopathology 2000;37:523–529.
[31] Pai SG, Carneiro BA, Mota JM, Costa R, Leite CA, Barroso-Sousa R, et al. Wnt/beta-catenin pathway: modulating anticancer immune response. J Hematol Oncol 2017;10:101.

[32] Augustin I, Dewi DL, Hundshammer J, Rempel E, Brunk F, Boutros M. Immune cell recruitment in teratomas is impaired by increased Wnt secretion. Stem Cell Res 2016;17:607–615.
[33] Spranger S, Gajewski TF. A new paradigm for tumor immune escape: beta-catenin-driven immune exclusion. J ImmunoTher Cancer 2015;3:43.
[34] The Cancer Genome Atlas Research Network. Comprehensive molecular characterization of gastric adenocarcinoma. Nature 2014;513:202–209.
[35] Wherry EJ, Kurachi M. Molecular and cellular insights into T cell exhaustion. Nat Rev Immunol 2015;15:486–499.
[36] Shen Y, Zhang S, Sun R, Wu T, Qian J. Understanding the interplay between host immunity and Epstein-Barr virus in NPC patients. Emerging Microbes Infect 2015;4 e20.
[37] Cho EY, Kim KH, Kim WS, Yoo KH, Koo HH, Ko YH. The spectrum of Epstein-Barr virus-associated lymphoproliferative disease in Korea: incidence of disease entities by age groups. J Korean Med Sci 2008;23:185–192.